

# Generation of superoxide anion and most likely singlet oxygen in irradiated TiO<sub>2</sub> nanoparticles modified by carotenoids

Tatyana A. Konovalova, Jesse Lawrence, Lowell D. Kispert\*

*Department of Chemistry, University of Alabama, Tuscaloosa, AL 35487-0336, USA*

Received 16 January 2003; received in revised form 22 May 2003; accepted 30 May 2003

## Abstract

Photosensitization of the TiO<sub>2</sub> nanoparticles with carotenoids leads to the formation of superoxide anion and singlet oxygen on red light irradiation. It has been shown that carotenoids facilitate generation of superoxide radical anion O<sub>2</sub><sup>•−</sup> in irradiated TiO<sub>2</sub> colloids. At low carotenoid concentrations (<3 × 10<sup>−5</sup> M) the rate constant of O<sub>2</sub><sup>•−</sup> production exceeds that obtained in the absence of carotenoid.

EPR experiments with 2,2,6,6-tetramethyl-4-piperidone and spin trapping with α-phenyl-*N*-*tert*-butyl nitron and 5,5-dimethyl-pyrroline-*N*-oxide showed that both superoxide anion and singlet oxygen can be produced in irradiated TiO<sub>2</sub> suspensions in toluene and CH<sub>2</sub>Cl<sub>2</sub>. The PBN–O<sub>2</sub><sup>•−</sup> and DMPO–O<sub>2</sub><sup>•−</sup> spin adducts were detected by the 9 GHz EPR/ENDOR spin trapping technique. The dismutation of superoxide radical anion was proposed to generate singlet oxygen through intermediate formation of HO<sub>2</sub><sup>•</sup> radicals. The PBN–HO<sub>2</sub><sup>•</sup> spin adduct was identified by the 9 GHz EPR/ENDOR and 95 GHz EPR spin trapping technique.

© 2004 Elsevier B.V. All rights reserved.

**Keywords:** Titanium dioxide; Carotenoids; Singlet oxygen; Superoxide radical anion; Electron paramagnetic resonance; Spin trapping

## 1. Introduction

The photocatalytic properties of titanium dioxide are well established. Photoexcitation of TiO<sub>2</sub> with an energy greater than its band gap (3.2 eV) results in the formation of active electron–hole pairs (e<sup>−</sup>h<sup>+</sup>) [1,2]. The photogenerated electrons react as reducing agents, whereas the concomitantly formed holes can function as potent oxidizing agents. The redox activity of TiO<sub>2</sub> has also a significant biological impact. It has been demonstrated that cellular nucleic acids, particularly RNA, can be oxidized by photoexcited TiO<sub>2</sub> [3]. This property of photoexcited TiO<sub>2</sub> could be useful for the photodynamic treatment of cancer [4,5]. This procedure relies on the irradiation of tumors with visible light following the uptake of a photosensitizer by the tumor tissue. The irradiated photosensitizer reacts with biomolecules or oxygen in its vicinity generating potent toxins such as singlet oxygen (<sup>1</sup>O<sub>2</sub>) or radicals resulting in cellular destruction [6–8]. Singlet oxygen and other reactive oxygen species (ROS) such as hydroxyl radical (•OH), superoxide radical anion (O<sub>2</sub><sup>•−</sup>) and hydrogen peroxide (H<sub>2</sub>O<sub>2</sub>) have been identified as the most prevalent reactive intermediates responsible for photochemical cell damage [9–12]. It has been postulated [13,14]

that in vivo <sup>1</sup>O<sub>2</sub> is produced by dismutation of superoxide anion in leukocytes.

With regard to the biomedical potential of TiO<sub>2</sub> it is important to examine the mechanism of ROS generation in photoexcited TiO<sub>2</sub> in the presence of photosensitizer. The most appropriate photosensitizer for the photodynamic therapy should have an ability to absorb red light because this wavelength penetrates human tissues. We are interested in the modification of TiO<sub>2</sub> with carotenoids because these natural dyes act as accessory light-harvesting pigments in the photosynthetic antenna complexes and have high extinction coefficients (>10<sup>5</sup> M<sup>−1</sup> cm<sup>−1</sup>) in the spectral region 450–650 nm [15]. It has been shown previously that modification of TiO<sub>2</sub> with carotenoids shifts the absorption threshold into the visible region and thus greatly improves the redox ability of the semiconductor [16].

Generation of ROS in photoexcited TiO<sub>2</sub> can be studied by means of electron paramagnetic resonance (EPR) spectroscopy. Formation of superoxide radical anion has been detected by the EPR spin-trapping technique upon photoexcitation of TiO<sub>2</sub> in ethanol [17]. Generation of singlet oxygen by irradiated titanium dioxide in methanol and aqueous solutions has been suggested [18,19]. Recently it has also been demonstrated that both <sup>1</sup>O<sub>2</sub> and O<sub>2</sub><sup>•−</sup> can be generated by irradiation of TiO<sub>2</sub> in ethanol and acetonitrile [20]. It has been reported that <sup>1</sup>O<sub>2</sub> production occurs in organic

\* Corresponding author. Tel.: +1-205-348-8436; fax: +1-205-348-9104.  
E-mail address: [lkispert@bama.ua.edu](mailto:lkispert@bama.ua.edu) (L.D. Kispert).

solvents in the presence of water where the concentration of  $O_2^{\bullet-}$  is not too large. When the concentration of  $O_2^{\bullet-}$  is larger, it can quench singlet oxygen [21]. The mechanism of singlet oxygen formation on irradiated  $TiO_2$  is still not clear.

In this study we used X-band (9 GHz) and W-band (95 GHz) EPR spectroscopy and electron nuclear double resonance (ENDOR) to detect and identify the oxygenated intermediates formed during the photoexcitation of  $TiO_2$  nanoparticles in organic solvents, and examine the influence of carotenoid molecules on their formation and quenching.

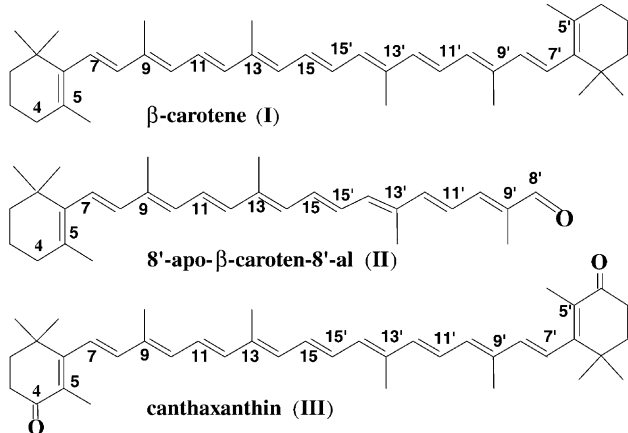
## 2. Experimental

### 2.1. Materials

Titanium oxide (anatase) nanoparticles (7 nm, ST-1) were obtained from the Ishihara Co. (Japan) and were used as received.  $\beta$ -Carotene (I) was supplied by Sigma, 8'-apo- $\beta$ -caroten-8'-al (II) by Roche Vitamins and Fine Chemicals, and canthaxanthin (III) by Fluka (see Scheme 1). Purity of the carotenoids was checked by  $^1H$  NMR (360 MHz,  $CDCl_3$ ) and TLC analyses. They were stored in the dark at  $-14^\circ C$  in a desiccator containing drierite. 2,2,6,6-Tetramethyl-4-piperidone (95%) was obtained from Aldrich and used as-received. The solvents  $CH_2Cl_2$  and toluene (Aldrich, anhydrous) were stored under an Ar atmosphere and used without further purification. The spin trap  $\alpha$ -phenyl-*N*-tert-butyl nitron (PBN, 98%) and free radical 4-oxo-TEMPO (TEMPONE) were purchased from Aldrich and stored in the dark at  $4^\circ C$ . The spin-trapping agent, purified 5,5-dimethyl-pyrroline-*N*-oxide (DMPO), was a gift from the National Institute of Environmental Health Science (NIEHS).

### 2.2. Sample preparation

All samples were freshly prepared.  $TiO_2$  (0.5 mg) was suspended in  $CH_2Cl_2$  or toluene solutions (0.2 ml) con-



Scheme 1.

taining 2,2,6,6-tetramethyl-4-piperidone ( $10^{-2}$  M) and a carotenoid ( $10^{-3}$  to  $10^{-5}$  M) and transferred to an EPR tube. For X-band (9.5 GHz) EPR measurements the samples were irradiated at room temperature directly in a microwave cavity with a light focused from a Xe/Hg lamp (1 kW) equipped with a Kratos monochromator. For ENDOR and W-band (95 GHz) EPR experiments irradiated samples were cooled to 77 K and stored at 77 K before use.

### 2.3. EPR measurements

EPR measurements at X-band (9.5 GHz) were carried out with a Varian E-12 EPR spectrometer, equipped with a rectangular cavity. The magnetic field was measured with a Bruker EPR 035M gaussmeter, and the microwave frequency was measured with a model HP 5245L frequency counter. ENDOR experiments were carried out with a Bruker ESR-300 EPR spectrometer, equipped with a DICE ENDOR facility. The W-band (95 GHz) measurements were performed with a Bruker E600 EPR spectrometer.

## 3. Results and discussion

### 3.1. EPR/ENDOR spin trapping

For detection of any possible paramagnetic intermediates in irradiated  $TiO_2$  suspensions in toluene or  $CH_2Cl_2$  an EPR spin-trapping technique was applied. Irradiation of  $TiO_2$  was carried out with light of energy higher than its band gap (350 nm). When  $TiO_2$  suspension in  $CH_2Cl_2$  or toluene was irradiated in the presence of PBN spin trap, the EPR spectrum measured at 9 GHz during irradiation at room temperature directly in a microwave cavity displayed overlapping signals arising from a mixture of spin adducts (Fig. 1a). Fig. 1 illustrates time-dependent changes in the spectrum. The resultant EPR spectrum measured after termination of

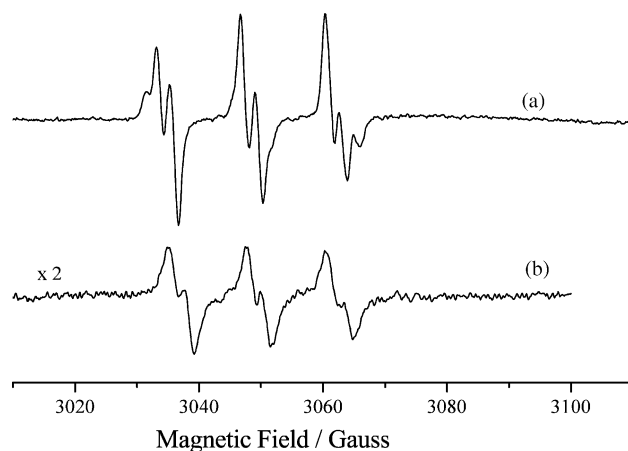


Fig. 1. EPR spectra of  $TiO_2$  colloids in toluene in the presence of PBN ( $2 \times 10^{-2}$  M) measured at room temperature: (a) during irradiation in situ; (b) 15 min after termination of irradiation.

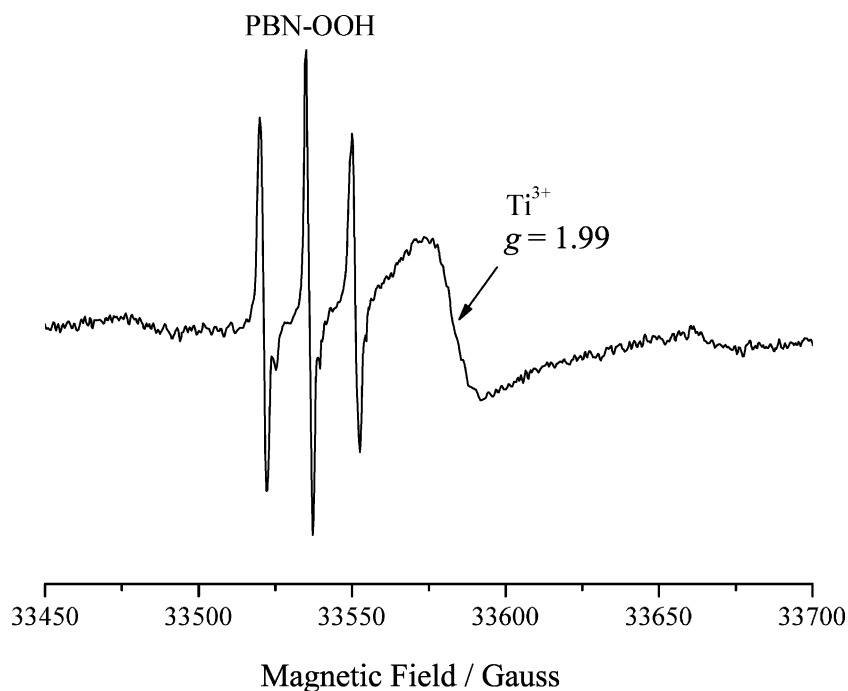
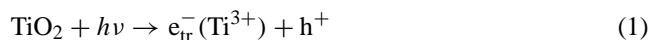


Fig. 2. W-band (95 GHz) EPR spectrum of a freshly prepared  $\text{TiO}_2$  colloids in toluene in the presence of PBN ( $2 \times 10^{-2}$  M) irradiated at room temperature, stored at 77 K, warmed to RT and measured at RT after 15 min. Scale is different than in Fig. 1.

irradiation ( $\sim 10$ – $15$  min), exhibits a triplet of doublets with hyperfine coupling constant (hfc)  $a_N = 14.2$  G and  $a_H = 2.8$  G that are similar to those of the PBN–OOH adduct (Fig. 1b). This signal is stable at room temperature. We also carried out 95 GHz (W-band) measurements at room temperature. It has been shown that high frequency EPR spectroscopy with enhanced  $g$  value resolution might be useful for separation and identification of spin adducts with similar  $g$  values [22]. From the W-band EPR spectrum of irradiated  $\text{TiO}_2$  with PBN, the PBN–OOH adduct stable at room temperature ( $a_N = 14.8$  G and  $a_H = 2.8$  G) was identified (Fig. 2). The spectrum exhibits also a broad line with  $g = 1.99$ . This signal has been assigned to the photogenerated electrons trapped as  $\text{Ti}^{3+}$  surface ions [23]:



At conventional 9 GHz frequency the  $\text{Ti}^{3+}$  signal was too broad to be observed. Recording the EPR spectrum at 95 GHz is particularly advantageous, since the broadening is significantly reduced, leading to higher spectral resolution. The differences in  $g$  values of any other PBN adducts were not large enough to be resolved.

For separation and detailed observation of the hfc of the trapped radicals produced by irradiated  $\text{TiO}_2$  colloids, ENDOR measurements were performed. When different spin adducts with similar hfc cannot be identified from their EPR spectra because of overlapping lines, the ENDOR technique makes the assignments possible because of the characteristic ENDOR pattern for each spin adduct [24,25]. Fig. 3 displays the ENDOR spectra of  $\text{TiO}_2$  colloids in  $\text{CH}_2\text{Cl}_2$

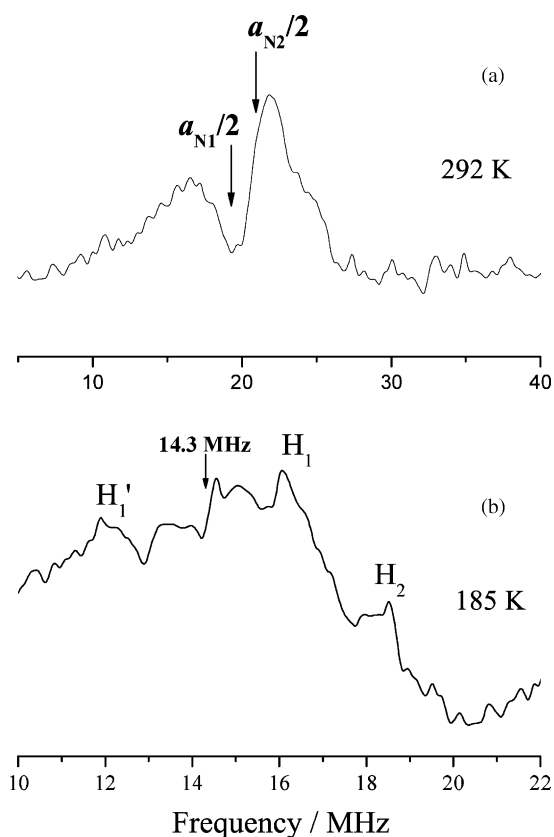


Fig. 3. ENDOR spectra of  $\text{TiO}_2$  colloids in toluene in the presence of PBN ( $2 \times 10^{-2}$  M) irradiated at 77 K and measured at: (a) 292 K ( $^{14}\text{N}$  ENDOR); (b) 185 K ( $^1\text{H}$  ENDOR).

in the presence of PBN irradiated at 77 K and measured at 292 K (a) and at 185 K (b). The  $^{14}\text{N}$  ENDOR spectrum at 292 K exhibits the features from two different spin adducts centered at  $a_{\text{N}1}/2$  and  $a_{\text{N}2}/2$ , respectively. In the case of a large hfc when  $a/2 > \nu_n$  ( $\nu_n$  is a Larmor nuclear frequency) the ENDOR features are centered around  $a/2$  ( $a_{\text{N}1}/2 = 19.32$  MHz and  $a_{\text{N}2}/2 = 20.7$  MHz) and separated by  $2\nu_n$  ( $\nu_n$  for  $^{14}\text{N}$  is 1.1 MHz). From the  $^{14}\text{N}$  ENDOR spectrum the hyperfine couplings  $a_{\text{N}1} = 38.64$  MHz (13.8 G) and  $a_{\text{N}2} = 41.4$  MHz (14.8 G) were determined.  $^1\text{H}$  ENDOR measured at 185 K revealed two proton doublets around the  $^1\text{H}$  Larmor frequency ( $\nu_{\text{H}} = 14.3$  MHz) with couplings  $a_{\text{H}1} = 4.9$  MHz (1.75 G) and  $a_{\text{H}2} = 7.96$  MHz (2.8 G). Two different spin adducts, the PBN/ $\text{O}_2^{\bullet-}$  ( $a_{\text{N}1} = 38.64$  MHz (13.8 G),  $a_{\text{H}1} = 4.9$  MHz (1.75 G)) [26–29] and PBN/ $\text{OOH}^{\bullet}$  ( $a_{\text{N}2} = 41.4$  MHz (14.8 G),  $a_{\text{H}2} = 7.96$  MHz (2.8 G)) [30,31], were identified on the basis of these results.

The formation of  $\text{O}_2^{\bullet-}$  in irradiated  $\text{TiO}_2$  has been confirmed by using the DMPO spin trap. The EPR spectrum measured after irradiation of  $\text{TiO}_2$  in toluene with DMPO exhibits a broad quartet (Fig. 4). Evaluated hyperfine coupling constants (hfc's)  $a_{\text{N}} = 13.65$  G and  $a_{\text{H}} = 10.6$  G suggest the generation of the superoxide anion adduct [17,32]. In the absence of  $\text{TiO}_2$ , irradiation of the DMPO toluene solution shows no signals.

We assume that  $\text{O}_2^{\bullet-}$  formation on irradiated  $\text{TiO}_2$  may occur as a result of both hole and electron trapping reactions. Photogenerated holes on  $\text{TiO}_2$  colloids could be trapped at lattice oxide ion sites as  $\text{O}^-$  species or as  $\bullet\text{OH}$  radicals at  $\text{OH}^-$  sites [33]. Pairwise trapping of holes as the diamagnetic  $\text{O}_2^{2-}$  ions has been proposed for  $\text{MgO}$  [34]. Adsorbed  $\text{O}_2^{2-}$  ions may produce  $\text{O}_2^{\bullet-}$  via reaction with both  $\text{h}^+$  or  $\bullet\text{OH}$ :

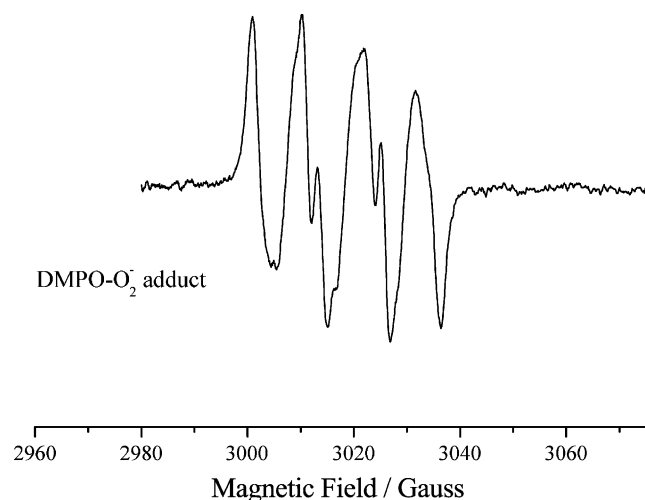


Fig. 4. EPR spectrum of the  $\text{DMPO-O}_2^{\bullet-}$  spin adduct (DMPO,  $5 \times 10^{-2}$  M) measured at RT in irradiated  $\text{TiO}_2$ .

On the other hand, the  $\text{O}_2^{\bullet-}$  formation can proceed through the reduction of molecular oxygen by the photogenerated electrons:



In the presence of water or OH groups in the system, the  $\bullet\text{OOH}$  formation has been reported [35].

### 3.2. Superoxide anion/singlet oxygen detection by use of 2,2,6,6-tetramethyl-4-piperidone

Another possible intermediate product of  $\text{TiO}_2$  irradiation is singlet oxygen. No direct method for identification of  $^1\text{O}_2$  is available to date. The indirect detection of singlet oxygen production by means of EPR spectroscopy is based on the formation of stable nitroxide radicals (NRs) when  $^1\text{O}_2$  reacts with sterically hindered amines [36,37]. Use of 2,2,6,6-tetramethyl-4-piperidone (4-oxo-TMP) as an  $^1\text{O}_2$  sensitive trapping agent has been reported [20,38]. However, this method is not specific for singlet oxygen. The superoxide anion can also contribute to the formation of NRs through the reaction with tertiary amines [39,40].

Irradiation of 2,2,6,6-tetramethyl-4-piperidone (4-oxo-TMP) solutions ( $2.5 \times 10^{-2}$  M) in  $\text{CH}_2\text{Cl}_2$  or toluene does not produce any EPR signals (Fig. 5a). However,  $\text{TiO}_2$  colloids in  $\text{CH}_2\text{Cl}_2$  or toluene containing 4-oxo-TMP when irradiated at 350 nm give rise to the triplet characteristic of NR (Fig. 5b) with  $a_{\text{N}} = 14.8$  G,  $g = 2.0061$  which are identical to those for stable TEMPONE radical. Fig. 5c

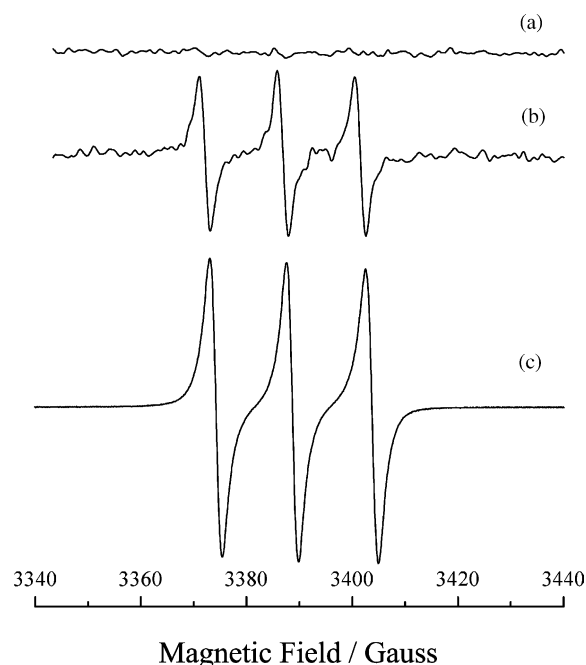
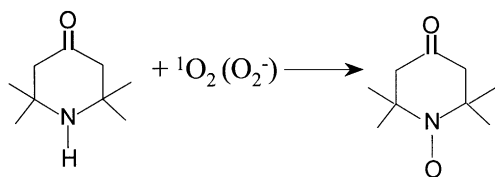


Fig. 5. EPR spectra of: (a) 4-oxo-TMP solution ( $10^{-2}$  M) in  $\text{CH}_2\text{Cl}_2$  irradiated at 77 K and measured at RT; (b) 4-oxo-TMP +  $\text{TiO}_2$  irradiated at 77 K and measured at RT; (c) TEMPONE solution in  $\text{CH}_2\text{Cl}_2$ ,  $a_{\text{N}} = 14.8$  G,  $g = 2.0061$ .



Scheme 2.

shows the EPR spectrum of TEMPONE in  $\text{CH}_2\text{Cl}_2$  solution. When experiments were carried out under oxygen eliminated conditions (in solutions deoxygenated with nitrogen) no nitroxide formation was detected. These observations verified that the TEMPONE signal comes from the reaction of 4-oxo-TMP with oxygen. It could be singlet oxygen or superoxide anion produced during photoexcitation of  $\text{TiO}_2$  colloids (Scheme 2).

Another possibility of the TEMPONE generation is the formation of N-centered radicals from TMP on irradiated  $\text{TiO}_2$  followed by triplet oxygen addition according to the mechanism reported by Roberts and Ingold [41]. However, studies of the production and the decay of singlet oxygen and superoxide anion in the presence of TMP and DMPO have shown that this pathway could be eliminated for generation of  $^1\text{O}_2$  [20].

The intensity of the NR signal as a function of the irradiation time is given in Fig. 6. The intensity increased with time, reached a plateau after  $\sim 10$  min of irradiation and then increased. The shape of the curve might suggest the accumulation of the  $\text{O}_2^{\bullet-}$  species at the beginning of the reaction followed by the  $^1\text{O}_2$  formation from superoxide anion.

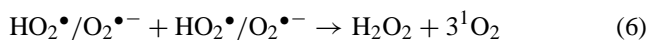
It has been shown [21,42] that in air-saturated organic solvents containing water superoxide anion can form perhy-

droxyl radicals  $\text{HO}_2^{\bullet}$  that are stronger oxidants than  $\text{O}_2^{\bullet-}$  according to the reaction:



It has been also reported that under UV illumination of the  $\text{TiO}_2/\text{O}_2$  system,  $\text{O}_2$  can react with  $\text{Ti}^{3+}\text{-OH}$  surface sites to make  $\text{HO}_2^{\bullet}$  species [41,43]. Generation of the  $\text{HO}_2^{\bullet}$  radicals on irradiated  $\text{TiO}_2$  was supported by our spin-trapping experiments.

In the absence of other reactants, the superoxide radical anion decays via the second-order reaction producing hydrogen peroxide and singlet oxygen [21,42]:



Hydrogen peroxide ( $\text{H}_2\text{O}_2$ ) has been detected as a concomitant reaction product of irradiated  $\text{TiO}_2$  in aqueous dispersions [44] and photodegradation of different dyes in the presence of  $\text{TiO}_2$  [45].

### 3.3. Irradiation of $\text{TiO}_2$ in the presence of carotenoids

We carried out irradiation of the  $\text{TiO}_2$  suspensions in  $\text{CH}_2\text{Cl}_2$  at 546 nm containing 4-oxo-TMP (0.5 mg of  $\text{TiO}_2 + 0.2$  ml of  $2.5 \times 10^{-2}$  M 4-oxo-TMP) in the presence of  $\beta$ -carotene (I), 8'-apo- $\beta$ -caroten-8'-al (II), and canthaxanthin (III) at different carotenoid concentrations (from  $10^{-3}$  to  $10^{-5}$  M). The  $\text{O}_2^{\bullet-}/^1\text{O}_2$  production was monitored by EPR measurements of the 4-oxo-TMPO signal at room temperature. When the concentration of 4-oxo-TMP was small enough and the EPR signal of nitroxide was not observed upon irradiation of  $\text{TiO}_2$  (Fig. 7a), addition of  $3 \times 10^{-5}$  M  $\beta$ -carotene resulted in the appearance of the nitroxide signal

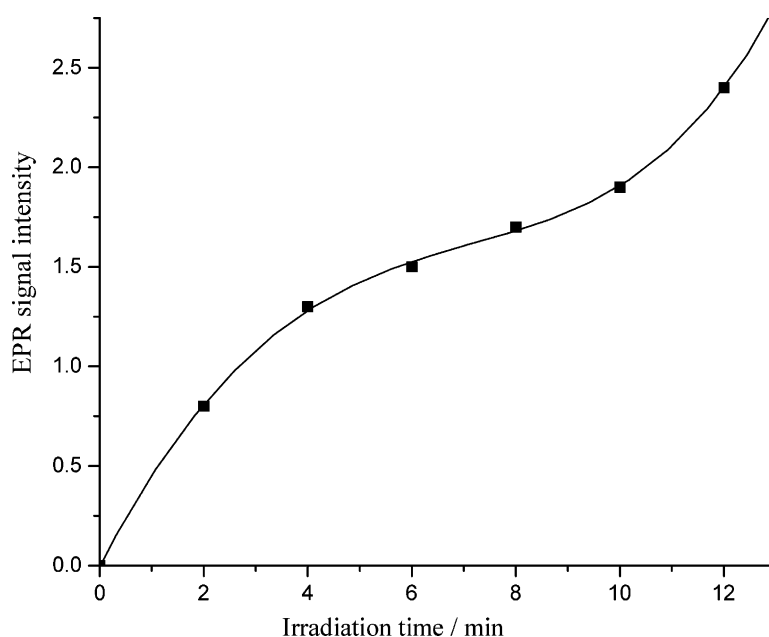


Fig. 6. Dependence of the NR signal observed in irradiated  $\text{TiO}_2/4$ -oxo-TMP on the irradiation time.

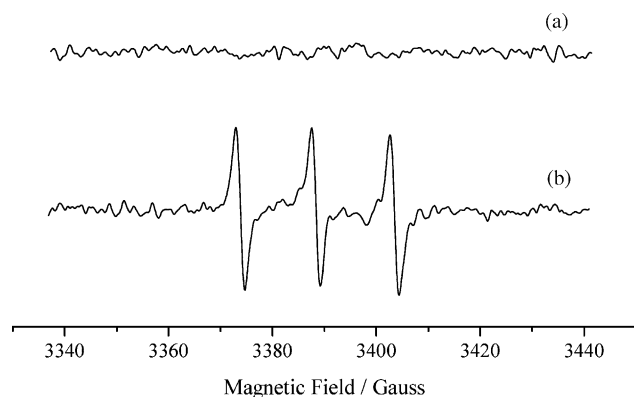


Fig. 7. EPR spectra of  $\text{TiO}_2$  in  $\text{CH}_2\text{Cl}_2$  + 4-oxo-TMP ( $2.0 \times 10^{-5}$  M) irradiated at 77 K: (a) without carotenoids; (b) in the presence of  $\beta$ -carotene.

(Fig. 7b). An enhancement of the nitroxide signal intensity was observed in the carotenoid concentration range from  $10^{-5}$  to  $10^{-4}$  M (signal intensities were normalized to a  $\text{Cr}^{3+}$  standard). At concentrations higher than  $1 \times 10^{-4}$  M carotenoids decrease the enhancement effect to a concentration dependent manner. The signal was eliminated completely by  $1.5 \times 10^{-3}$  M  $\beta$ -carotene. Fig. 8 shows the dependence of the NR formation on the  $\beta$ -carotene concentration, where  $I_0$  is the intensity of the EPR signal of the NR in the absence of the carotenoid and  $I$  that in the presence of the carotenoid. An increase in the NR signal intensity could be due to a line width narrowing because of  $\text{O}_2^{\bullet-}$  consumption by carotenoids. However, no change of the nitroxide signal line width was detected in the presence of carotenoids.

It is well known that carotenoids are powerful quenchers of singlet oxygen [13]. It has been reported that singlet

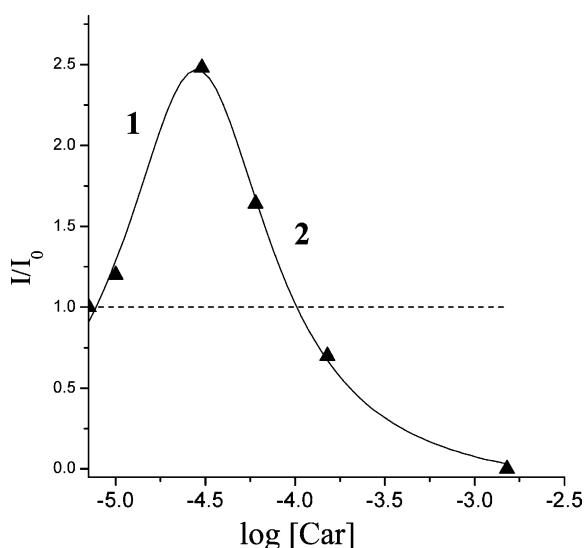
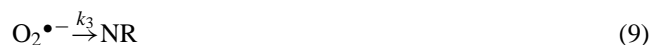
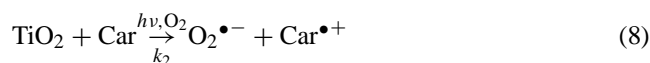


Fig. 8. NR formation in irradiated  $\text{TiO}_2$ /4-oxo-TMP in the presence of  $\beta$ -carotene as a function of the log carotenoid concentration at  $[\text{Car}] = 0$  M,  $[\text{Car}] = 1 \times 10^{-5}$  M,  $[\text{Car}] = 3 \times 10^{-5}$  M,  $[\text{Car}] = 6 \times 10^{-5}$  M,  $[\text{Car}] = 1.5 \times 10^{-4}$  M,  $[\text{Car}] = 1.5 \times 10^{-3}$  M.

oxygen is quenched very effectively by low concentrations of carotenoids [14,46]. For instance, 95% of  $^1\text{O}_2$  is inhibited by  $10^{-4}$  M  $\beta$ -carotene [14]. The rate constants for the quenching of  $^1\text{O}_2$  in toluene solutions by  $\beta$ -carotene and canthaxanthin are  $(1.3\text{--}1.4) \times 10^{10} \text{ M}^{-1} \text{ s}^{-1}$  [47]. This is at the order of magnitude greater than the carotenoid scavenging rates for oxygen radicals ( $\sim 10^9 \text{ M}^{-1} \text{ s}^{-1}$ ) [48]. Assuming that carotenoids can quench  $^1\text{O}_2$  effectively even at low concentrations ( $10^{-5}$  to  $10^{-4}$  M), and an increase of the NR intensity in Fig. 8 is mostly due to  $\text{O}_2^{\bullet-}$  generation followed by the reaction with TMP, we can estimate the relative rates of the  $\text{O}_2^{\bullet-}$  production in the presence and absence of carotenoids. The following reactions are considered:



where  $k_1$  is the rate constant of the formation of  $\text{O}_2^{\bullet-}$  in the absence of a carotenoid;  $k_2$  that in the presence of a carotenoid;  $k_3$  the rate constant of the nitroxide formation and  $k_4$  the rate constant of  $\text{O}_2^{\bullet-}$  trapping by carotenoid, where P is the Car- $\text{OO}^{\bullet}$  spin adduct.

The kinetics of these reactions would be

$$\frac{d[\text{O}_2^{\bullet-}]_0}{dt} = k_1 - k_3 \quad (11)$$

$$\frac{d[\text{O}_2^{\bullet-}]}{dt} = k_1 + k_2[\text{Car}] - k_3 - k_4[\text{Car}] \quad (12)$$

$$\frac{d[\text{O}_2^{\bullet-}]}{d[\text{O}_2^{\bullet-}]_0} = \frac{k_1 - k_3 + (k_2 - k_4)[\text{Car}]}{k_1 - k_3} \quad (13)$$

Assuming that the concentration of  $\text{O}_2^{\bullet-}$  in the presence of a carotenoid,  $[\text{O}_2^{\bullet-}]$ , corresponds to  $I$ , and that in the absence of a carotenoid  $[\text{O}_2^{\bullet-}]_0$  to  $I_0$ , and  $k_4$  is negligible at low carotenoid concentrations (part 1 of the curve in Fig. 8), we can simplify the kinetics:

$$\frac{dI}{dI_0} = 1 + \frac{k_2}{k_1 - k_3} [\text{Car}] \quad (14)$$

It is well known that the  $\text{O}_2^{\bullet-}$  species generated electrochemically in aprotic solvents is relatively stable [49]. This is in agreement with the stability of  $\text{O}_2^{\bullet-}$  generated photolytically in the  $\text{TiO}_2/\text{O}_2$  system [50] and observed by means of EPR by Anpo et al. [51]. Because of the sufficient stability of the  $\text{O}_2^{\bullet-}$  species on  $\text{TiO}_2$ , a rapid chemical reaction between  $\text{O}_2^{\bullet-}$  and TMP can be excluded. Thus, we assume that  $k_1 \gg k_3$ . In this case a first-order plot of  $I/I_0$  vs.  $[\text{Car}]$  results in a slope of  $(k_2/k_1)$  (see Fig. 9). The estimated ratio  $k_2/k_1 = (5.0 \pm 0.3) \times 10^4 \text{ M}^{-1}$ . Thus, at low carotenoid concentrations the rate constant of  $\text{O}_2^{\bullet-}$  production exceeds

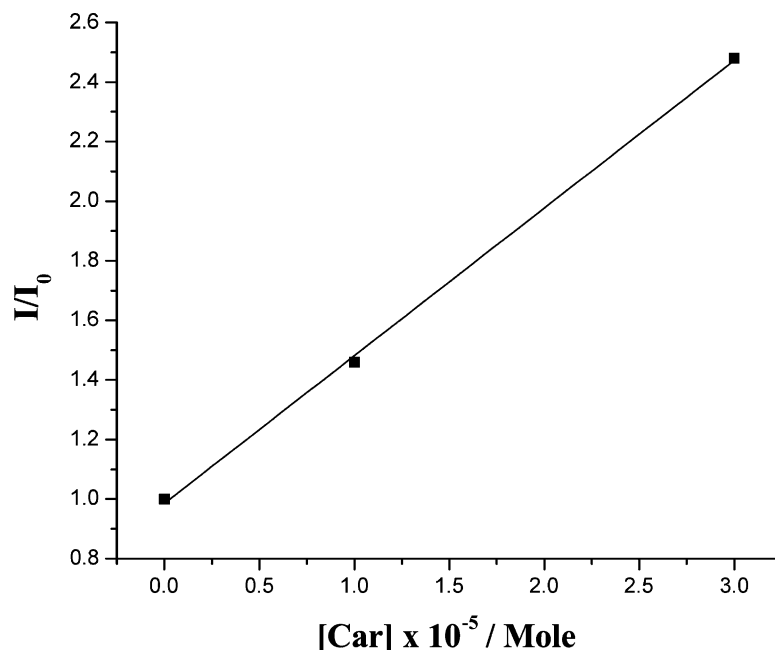
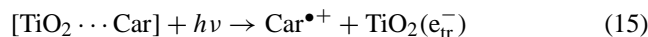
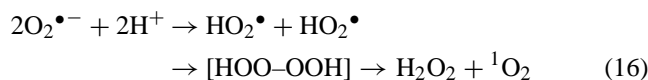


Fig. 9. Dependence of the ratio of the nitroxide EPR intensities on the concentration of carotenoid. Carotenoid concentrations: 0.0,  $1 \times 10^{-5}$ ,  $3 \times 10^{-5}$  M.

that obtained in the absence of carotenoid. This is in accordance to our previous studies which showed that irradiation of the TiO<sub>2</sub> colloids modified by carotenoids [16] greatly increases charge separation between the photogenerated holes trapped at the carotenoid as radical cations Car<sup>•+</sup> and the electrons trapped on the surface as TiO<sub>2</sub>(e<sub>tr</sub><sup>-</sup>):



This facilitates electron transfer to the adsorbed molecular oxygen according to reaction (4). The possible mechanism of <sup>1</sup>O<sub>2</sub> generation on irradiated TiO<sub>2</sub> colloids is based on dismutation of superoxide anion



It should be mentioned that the standard free energy of 37.5 kcal reported for this reaction [52] provides sufficient energy for the generation of singlet oxygen.

We cannot also exclude that singlet oxygen might be generated directly from triplet oxygen on the irradiated TiO<sub>2</sub> surface.

#### 4. Conclusions

Our EPR experiments showed that superoxide anion and, most likely, singlet oxygen can be produced in irradiated TiO<sub>2</sub> suspensions in toluene and CH<sub>2</sub>Cl<sub>2</sub>. The PBN–O<sub>2</sub><sup>•-</sup> and DMPO–O<sub>2</sub><sup>•-</sup> spin adducts were detected by the 9 GHz EPR/ENDOR spin-trapping technique. The dismutation of superoxide radical anion was proposed to generate singlet

oxygen through intermediate formation of HO<sub>2</sub><sup>•</sup> radicals. The PBN–HO<sub>2</sub><sup>•</sup> spin adduct was identified by the 9 GHz EPR/ENDOR and 95 GHz EPR spin-trapping technique.

It was shown that carotenoids act as photosensitizers for the TiO<sub>2</sub> colloids shifting the absorption band to the longer wavelengths and able to generate the O<sub>2</sub><sup>•-</sup> and <sup>1</sup>O<sub>2</sub> on visible light (550 nm) irradiation. Photosensitization of TiO<sub>2</sub> by carotenoids facilitates generation of the superoxide radical anion O<sub>2</sub><sup>•-</sup>. At low carotenoid concentrations (<3 × 10<sup>-5</sup> M) the rate constant of O<sub>2</sub><sup>•-</sup> production exceeds that obtained in the absence of carotenoid.

It was demonstrated that the photosensitization of titanium dioxide with carotenoids is sufficient to improve the biomedical potential of TiO<sub>2</sub>.

#### Acknowledgements

This work was supported by the US Department of Energy, Chemical Sciences, Geosciences and Biosciences Division, Office of Science, Office of Basic Energy Sciences, Grant DE-FG02-86ER13465. The NSF MRI Program is acknowledged for the acquisition of the W-band EPR spectrometer through grant CHE-0079498.

#### References

- [1] D. Duonghong, J. Ramsden, M. Gratzel, *J. Am. Chem. Soc.* 104 (1982) 2977.
- [2] G. Rothenberger, J. Moser, M. Gratzel, N. Serpone, D.K. Sharma, *J. Am. Chem. Soc.* 107 (1985) 8054.

- [3] W.G. Wamer, J.-J. Yin, R.-R. Wei, *Free Rad. Biol. Med.* 23 (1997) 851.
- [4] R. Cai, K. Hashimoto, K. Itoh, Y. Kubota, A. Fujishima, *Bull. Chem. Soc. Jpn.* 64 (1991) 1268.
- [5] R. Cai, Y. Kubota, T. Shuin, H. Sakai, K. Hashimoto, A. Fujishima, *Cancer Res.* 52 (1992) 2346.
- [6] T.J. Dougherty, *Photochem. Photobiol.* 58 (1993) 895.
- [7] J. Moan, K. Berg, *Photochem. Photobiol.* 55 (1992) 931–948.
- [8] B.W. Henderson, T.J. Dougherty, *Photochem. Photobiol.* 55 (1992) 145.
- [9] K. Briviba, L.O. Klotz, H. Sies, *Biol. Chem.* 378 (1997) 1259.
- [10] C. Richter, J.W. Park, B.N. Ames, *Proc. Natl. Acad. Sci. USA* 85 (1988) 6465.
- [11] T. Grune, L.O. Klotz, J. Gieche, M. Rudeck, H. Sies, *Free Rad. Biol. Med.* 30 (2001) 1243.
- [12] M. Geoffroy, P. Lambelet, P. Richert, *J. Agric. Food Chem.* 48 (2000) 974.
- [13] N.I. Krinsky, *Science* 186 (1974) 363.
- [14] S.C. Foote, R.W. Denny, *J. Am. Chem. Soc.* 90 (1968) 6233.
- [15] Y. Koyama, *J. Photochem. Photobiol. B* 9 (1991) 265.
- [16] T.A. Konvalova, V.V. Konvalov, L.D. Kispert, *J. Phys. Chem. B* 103 (1999) 4672.
- [17] H. Noda, K. Oikawa, H. Ohya-Nishiguchi, H. Kamada, *Bull. Chem. Soc. Jpn.* 66 (1993) 3542.
- [18] W.C. Dunlap, Y. Yamamoto, M. Inoue, M. Kashiba-Iwatsuki, M. Yamaguchi, K. Tomita, *Int. J. Cosmetic Sci.* 20 (1998) 1.
- [19] S.P. Pappas, R.M. Fisher, *J. Paint Technol.* 46 (1974) 65.
- [20] R. Konaka, E. Kashahara, W.C. Dunlap, Y. Yamamoto, K. Chien, M. Inoue, *Free Rad. Biol. Med.* 27 (1999) 294.
- [21] A.U. Khan, *J. Am. Chem. Soc.* 99 (1977) 370.
- [22] T.I. Smirnova, A.I. Smirnov, R.B. Clarkson, R.L. Belford, Y. Kotake, E.G. Janzen, *J. Phys. Chem. B* 101 (1997) 3877.
- [23] R.F. Howe, M. Grätzel, *J. Phys. Chem.* 89 (1985) 4495.
- [24] E.G. Janzen, U.M. Oehler, D.L. Haire, Y. Kotake, *J. Am. Chem. Soc.* 108 (1986) 6858.
- [25] Y. Kotake, M. Okazaki, K. Kuwata, *J. Am. Chem. Soc.* 99 (1977) 5198.
- [26] N. Ohto, E. Niki, Y. Kamiya, *J. Chem. Soc., Perkin Trans. II* (1977) 1770.
- [27] E. Niki, S. Yokoi, J. Tsuchiya, Y. Kamiya, *J. Am. Chem. Soc.* 105 (1983) 1498.
- [28] W.A. Pryor, D.G. Prier, D.F. Church, *J. Am. Chem. Soc.* 105 (1983) 2883.
- [29] M.V. Merritt, R.A. Johnson, *J. Am. Chem. Soc.* 99 (1977) 3713.
- [30] J.R. Harbour, V. Chow, J.R. Bolton, *Can. J. Chem.* 52 (1974) 3549.
- [31] C.D. Jaeger, A.J. Bard, *J. Phys. Chem.* 83 (1979) 3146.
- [32] J.R. Harbour, M.L. Hair, *J. Phys. Chem.* 81 (1977) 1791.
- [33] O.I. Micic, Y. Zhang, K.R. Cromack, A.D. Trifunac, M.C. Thurnauer, *J. Phys. Chem.* 97 (1993) 7277.
- [34] B.V. King, F. Freund, *Phys. Rev. B* 29 (1984) 5814.
- [35] X. Fu, W.A. Zeltner, M.A. Anderson, *Stud. Surf. Sci. Catal.* 103 (1996) 445.
- [36] Y. Lion, M. Delmelle, A. van de Vorst, *Nature* 263 (1976) 442.
- [37] J. Moan, E. Wold, *Nature* 279 (1979) 450.
- [38] A. Viola, C. Hadjur, A. Jeunet, M. Julliard, *J. Photochem. Photobiol. B* 32 (1996) 49.
- [39] R. Poupko, I. Rosenthal, *J. Phys. Chem.* 77 (1973) 1722.
- [40] G.M. Rosen, E. Finkelstein, E.J. Rauckman, *Arch. Biochem. Biophys.* 215 (1982) 367.
- [41] J.R. Roberts, K.U.J. Ingold, *Am. Chem. Soc.* 95 (1973) 3228.
- [42] R. Zhang, S. Goldstein, A. Samuni, *Free Rad. Biol. Med.* 26 (1999) 1245.
- [43] C. Kormann, D.W. Bahnemann, M.R. Hoffmann, *J. Phys. Chem.* 92 (1988) 5196.
- [44] J.R. Harbour, J. Tromp, M.L. Hair, *Can. J. Chem.* 63 (1985) 204.
- [45] T. Wu, G. Liu, J. Zhao, H. Hidaka, N. Serpone, *J. Phys. Chem. B* 103 (1999) 4862.
- [46] S.C. Foote, Y.C. Chang, R.W. Denny, *J. Am. Chem. Soc.* 92 (1970) 3216.
- [47] P.F. Conn, W. Schalch, T.G. Truscott, *J. Photochem. Photobiol.* 11 (1991) 41.
- [48] N.E. Polyakov, A.I. Kruppa, T.V. Leshina, T.A. Konvalova, L.D. Kispert, *Free Rad. Biol. Med.* 31 (2001) 43.
- [49] D.T. Sawyer, K. Yamaguchi, T.S. Calderwood, in: R.A. Greenwald (Ed.), *Handbook of Methods for Oxygen Radical Research*, CRC Press, Boca Raton, FL, 1986, p. 65.
- [50] M.A. Henderson, W.S. Epling, C.H.F. Peden, C.L. Perkins, *J. Phys. Chem. B* 107 (2003) 534.
- [51] M. Anpo, M. Aikawa, Y. Kubokawa, M. Che, C. Louri, O.E. Cramell, *J. Phys. Chem.* 89 (1985) 5594.
- [52] W.M. Latimer (Ed.), *Oxidation Potentials*, 2nd ed., Prentice-Hall, New York, 1952.